HU Protein Induces Incoherent DNA Persistence Length

Guy Nir,[†‡] Moshe Lindner,[†‡] Heidelinde R. C. Dietrich,[§] Olga Girshevitz,[‡] Constantinos E. Vorgias,[¶] and Yuval Garini[†‡*]

[†]Physics Department and [‡]Institute for Nanotechnology, Bar Ilan University, Ramat-Gan, Israel; [§]Department of Imaging Science and Technology, Delft University of Technology, Delft, The Netherlands; and [¶]Department of Biochemistry and Molecular Biology, Faculty of Biology, National and Kapodistrian University of Athens, Athens, Greece

ABSTRACT HU is a highly conserved protein that is believed to play an important role in the architecture and dynamic compaction of bacterial DNA. Its ability to control DNA bending is crucial for functions such as transcription and replication. The effects of HU on the DNA structure have been studied so far mainly by single molecule methods that require us to apply stretching forces on the DNA and therefore may perturb the DNA-protein interaction. To overcome this hurdle, we study the effect of HU on the DNA structure without applying external forces by using an improved tethered particle motion method. By combining the results with DNA curvature analysis from atomic force microscopy measurements we find that the DNA consists of two different curvature distributions and the measured persistence length is determined by their interplay. As a result, the effective persistence length adopts a bimodal property that depends primarily on the HU concentration. The results can be explained according to a recently suggested model that distinguishes single protein binding from cooperative protein binding.

INTRODUCTION

Nucleoid-associated proteins (NAPs) together with macromolecular crowding effects play a major role in maintaining the architecture of the bacterial chromosome. NAPs' ability to control the DNA structure is prominent for their role as regulators of DNA translocations (1–5). One of the most abundant NAPs is HU, a histonelike DNA binding protein initially identified and characterized in *Escherichia coli* strain U93. In several enterobacteria, such as *E. coli*, the HU (*Eco*HU) is a heterodimer with a molecular mass of ~19 kDa, whereas in most bacteria HU is a homodimer (2). HU is known for its DNA bending activity and binds DNA in a nonspecific manner, although several studies have shown that the protein binds to distorted DNA with a higher binding affinity (6–8). The bending activity is crucial for functions such as transcription regulation (9,10) and replication (11,12). It was also found that cells lacking HU are extremely sensitive to γ- and ultraviolet irradiation (10,13), which suggests that HU is involved in DNA repair.

Recent single molecule experiments based on tweezers (14–16) or fluorescence resonance energy transfer (17) examined the bending activity of *Eco*HU and *Bacillus stearothermophilus* HU (*Bst*HU) proteins. They showed a bimodal behavior induced by HU on the DNA. At low HU concentrations up to a salt concentration of 100 mM NaCl (18), it decreases the persistence length, thereby making the DNA more flexible and compact; but at high HU concentrations it increases the persistence length, making the DNA stiffer and less compact than HU-free DNA.

These previous single molecule experiments mainly used magnetic tweezers techniques in which a magnetic particle is tethered through DNA to the surface and a magnetic force is applied on the bead, stretching it upward. The DNA extension is measured as a function of the stretching force and the persistence length is determined by fitting the data to the relevant model. Detailed force-extension measurements of individual polymers, in particular of nucleic acids, opened up the possibility of investigating their properties and interactions with structural proteins and molecular motors, to name but a few, and yielded highly valuable data (19–23).

Nevertheless, the intrinsic application of force on the DNA might in some cases introduce perturbations on its natural conformation and modify its interaction properties with proteins (24,25). New theoretical models to the bimodal behavior were also described lately (26–28) and can be compared with experimental results.

Based on the importance of HU-DNA interaction and the lack of experimental data for DNA at its natural form, we studied in this work the effect of HU on DNA and tested the validity of the theoretical model with two complementary techniques, tethered particle motion (TPM) (29–36) and atomic force microscopy (AFM) (37,38). TPM is a single-molecule method that allows us to study the mechanical properties of polymers such as DNA, and its interaction with proteins. TPM is advantageous, inasmuch as it does not require us to apply forces on the studied polymer. AFM allows revealing direct structural information on the HU-DNA complexes, although it is neither a dynamic nor a force-free method. In TPM, one end of the polymer is attached to the surface whereas the other is bound to a marker that can be detected with high spatial precision. By following the distribution of the marker position, the

Submitted October 6, 2010, and accepted for publication December 2, 2010.

*Correspondence: gariniy@mail.biu.ac.il

Editor: Laura Finzi.

0006-3495/11/01/0001/7 $2.00

doi: 10.1016/j.bpj.2010.12.3687

Please cite this article in press as: Nir et al., HU Protein Induces Incoherent DNA Persistence Length, Biophysical Journal (2011), doi:10.1016/j.bpj.2010.12.3687

mechanical properties of the polymer can be deduced, as well as deviations therein that results from interactions with proteins or environmental changes. TPM does not require us to apply forces on the studied polymer—enabling us to study protein-DNA interactions in a way that better imitates the natural conditions of the interaction.

In the tethered-based methods, one finds the distribution of the end-to-end distance of the polymer. It depends on the contour length and the persistence length of the polymer (39), but there are no details of the microscopic mechanism because the end-to-end distance itself is an average value. We therefore also used AFM as a complementary technique. AFM measurements, in contrast to tethered-based methods, provide direct information on the two-dimensional projection of the polymer (38) and reveal its curvature along the contour length. Therefore, more delicate features that go beyond the single-parameter-based models of a polymer can be identified.

Primarily we measured the variations of single double-stranded DNA (dsDNA) persistence length as a function of different concentrations of HU protein using an optimized TPM method, as explained below. To the best of our knowledge, this is the first time that TPM is being used to calculate the persistence length in a protein-DNA interaction study by observing the gradual changes of the DNA persistence length. The results indicate the coexistence of two different conformations along a single DNA, although the end-to-end distance can still be described with a single effective persistence length.

The TPM setup consisted of a dark-field microscope, an EM-CCD (see Materials and Methods) and the DNA is marked at its end with a gold nanobead (diameter of 80 nm). The small size of the bead with respect to the DNA contour length and its bright scattering signal plays a key factor for the accuracy of the collected data.

Firstly, it ensures that the bead acts as a passive probe of the polymer dynamics. This criterion is met when the excursion number,

$$N_r = R/\sqrt{L\xi/3} < 1,$$

defined as the ratio of the bead radius R to the radius of gyration of DNA, is smaller than unity. For dsDNA with a contour length of $L = 925$ nm, a known persistence length of $\xi = 50$ nm for bare DNA, and a gold bead with $r = 40$ nm, the excursion number is $N_r \sim 0.32$, which meets the criterion (30,40).

Secondly, the plasmon scattering from the small gold bead provides an intense signal, which enables us to measure bright time-lapse images of the bead movement with low exposure times (1–2 ms) and high frame rate. It leads to a more accurate determination of the bead position during the single particle analysis and minimizes blurring. Although blurring due to long exposure times can be corrected (41,42), it increases the error and better be avoided.

MATERIALS AND METHODS

Protein

The recombinant HU from *Bacillus stearothermophilus* was produced in BL21(DE3)pLysS and purified to highest purity using Heparin-Sepharose and SP-Sepharose as described in Padas et al. (43). The purity and its native conformation were verified by sodium dodecyl sulfate polyacrylamide gel electrophoresis according to Laemmli and circular dichroic spectroscopy, respectively. The concentration of HU was measured at 230 nm using 1 mg/mL = 0.6 OD.

DNA constructs

We synthesized dsDNA fragments from unmethylated λ-DNA template (Promega, Madison, WI) using a polymerase chain reaction to achieve fragments of 2.7 kb with the following primers (Isogen, De Meern, The Netherlands):

5′-Biotin-ATA GGC CAG TCA ACC AGC AGG-3′ (forward),

5′ DIG-GGG ATA ATC GGC GTG GCA GAT AAC-3′ (reverse).

Biotin and digoxigenin were attached at the opposite ends of the DNA strands to tether it at one end to an anti-biotin conjugated nanobead (BBI, Cardiff, UK) and at the other end to an anti-digoxigenin (Roche, Basel, Switzerland) coated surface. Beads with a diameter of 80 nm were used.

TPM experiments

Preparation of flow chamber

All experiments were performed in a flow cell made out of two cover glasses (~150 μm thickness). Two holes (diameter of 1.5 mm) were laser-drilled in one cover glass to enable injection of reagents and buffers. For cleaning the slides, they were sonicated for 20 min first with 5% Alconox (Alconox, White Plains, NY), followed with ddw (5 min) acetone and finally ethanol.

The flow chamber has a volume of ~40 μL. It was constructed using two 170-μm-thick slides sandwiched with a ~150-μm-thick Parafilm (Pechiney Plastic Packaging, Chicago, IL) that was cut in the middle to create the flow channel.

Tethering the DNA

First, we prepared a mix solution containing 5 mg/mL blotting grade blocker (Bio-Rad, Haifa, IL) and 50 μg/mL anti-digoxigenin in phosphate-buffered saline (PBS buffer; Biological Industries, Beit Haemek, IL) and incubated it for 45 min. After incubation, the excess mix solution was washed with PBS buffer.

Another solution containing 50 μg/mL anti-digoxigenin in PBS was introduced into the flow cell and incubated for 45 min. The excess antibody was then removed by washing the chamber with 0.2 mL PBS buffer. Then 0.2 mL of PB buffer (50 mM sodium phosphate buffer, PH 7.5 containing 50 mM NaCl, 10 mM EDTA, and 0.02% Tween) containing DNA at a concentration of 3 μg/mL and 1 mg/mL Bio-Rad blotting grade blocker was introduced into the flow chamber and incubated for 60 min. Unbound DNA was removed by washing with PB buffer. Anti-biotin-coated gold nanobeads (80-nm diameter; BBI) diluted in PB buffer were then introduced into the chamber and allowed to incubate for 60 min.

Free nanobeads were removed from the flow chamber by washing with 0.3 mL of PB buffer. The whole procedure was performed in room temperature.

Please cite this article in press as: Nir et al., HU Protein Induces Incoherent DNA Persistence Length, Biophysical Journal (2011), doi:10.1016/j.bpj.2010.12.3687

Data collection

The DNA conformation changes randomly in the solution and its end-to-end distance is measured by finding the position of the bead. Although the bead is small (diameter of 80 nm), the plasmon scattering from such a bead is intense enough even at short exposure times such as 1 ms.

The experimental setup consists of a dark-field microscope unit (BX-RLA2; Olympus, Tokyo, Japan) with a ×50 objective lens (NA = 0.8) and an EM-CCD camera (DU-885; Andor, Belfast, Northern Ireland) with a pixel size of 8 × 8 μm and a maximal pixel read-out rate of 35 MHz (30). We collect at least 13 sets for each DNA molecule (a total of 18 dsDNA molecules) for each HU concentration. Each set is consisted of 1250–2500 frames. The exposure time for each frame was in the range of 1–3 ms and provided high-enough signal/noise ratio for accurate single particle tracking. With this exposure time, and by limiting the region of interest that is measured, a frame rate of 80–180 Hz is achieved.

Data analysis

The data was analyzed with a software package developed in our lab for single particle tracking with MATLAB (The MathWorks, Natick, MA) and further extraction of the DNA persistence length from the distribution.

First, we extract the bead position coordinates $x(t)$, $y(t)$ (two-dimensional projection) for each image (t).

Then the radial distribution $P(r)$ is calculated and fitted to the expected distribution according to the freely jointed chain model, which gives the Rayleigh distribution of

$$P_{2D}(r)dr = \frac{3}{4\pi L\xi}\cdot\exp\left(-\frac{3r^2}{4L\xi}\right)\cdot 2\pi r\cdot dr,$$

where L is the known contour length and ξ is the persistence length, which serves as a single fitting parameter (see the Supporting Material for more information).

AFM measurements

The actual conformations along the DNA strand were found by measuring the DNA with AFM. It was demonstrated before that the flattened DNA are equilibrated on a mica surface as in an ideal two-dimensional solution (38). Here we measured the curvatures of the DNA after it was hybridized with different concentration of HU protein at the same conditions as used during the TPM experiments.

Sample preparation

Samples were prepared in buffer solution containing 7.5 mM HEPES, 10 mM NaCl, and 3 mM $NiCl_2$. For naked DNA and 250 nM HU-DNA complex, we used 1–3 ng/μL DNA and for 1000 nM HU-DNA complex, we used 5 ng/μL DNA due to unspecific binding of unbound protein to the mica surface. After 30 min of incubation with HU (250 nM and 1 μM), muscovite mica (Bar-Naor, Ramat Gan, Israel) was cleaved and the sample was deposited on it. After 5 min of incubation it was rinsed with Milli-Q water (15–20 mL; Millipore, Billerica, MA), quickly dried (with Kim wipes and then blow-dried), and imaged.

Imaging samples

For imaging, we used Nanoscope V atomic force microscope (Veeco Instruments, Santa Barbara, CA). Images were acquired in tapping mode in air, with a number of scan sizes (indicated at each figure) using TESP-SS silicon tips (Veeco Instruments) with a spring constant of 42 N/m, frequency 320 kHz, and tip radius 2–5 nm.

Data analysis

The analysis is performed in two parts. Initial analysis is done with Gwyddion software (http://gwyddion.net/) and includes data leveling, removing polynomial background, and correcting lines and scars. After that, the DNA strands are analyzed with adequate software written in our lab (MATLAB).

For each DNA strand, we compute the curvature distribution.

First, we define a contour line along each DNA strand.

We then subtract the background, calculate the end-to-end distance, and find the curvature κ using 10-nm segments along the DNA. This value is selected to be larger than the size of a protein that is bound to the DNA, but smaller than a typical curve along the DNA (i.e., the persistence length). The curvature is calculated by finding the angle difference $\Delta\theta$ of each two neighbor-segments and dividing by the segment length. The angle of each segment along the DNA is found using

$$\theta = \operatorname{atan}\left(\frac{y_2 - y_1}{x_2 - x_1}\right)\cdot\frac{180}{\pi},$$

where x_1, y_1 and x_2, y_2 are the coordinates of the segment edges. The cumulative distribution function (CDF) is calculated from the distribution of the angles. We analyzed fifty-nine naked DNA molecules, thirty 250-nM HU-DNA complexes, and twenty-two 1000-nM HU-DNA complexes.

RESULTS AND DISCUSSION

For measuring the properties of a dsDNA at different HU concentrations, we start by allocating a tethered bead and measure its spatial distribution (at least 1500 time-frames). To ensure that the bead is appropriately tethered through a single double-stranded DNA, we initially measured the properties of the DNA in protein-free buffer solution and extracted the persistence length. The detailed acquisition procedures are described in Materials and Methods, and the data analysis procedure for extracting the persistence length is described in the Supporting Material. The typical calculated persistence length for those molecules that passed the criteria (refer to Supporting Material) is found to be 50 ± 10 nm (±6 nm in 82% of the data). We then measured the end-to-end distribution for the same DNA molecule with different HU concentrations in the range of 5 nM to 3 μM. The protein concentration was changed every 30 min by injecting a volume of 0.2 mL of the new HU concentration to the chamber, which is ~5 times larger than the chamber volume. It ascertained that the chamber content was fully replaced with the new concentration.

The dependence of the DNA persistence length on HU concentration is shown in Figs. 1–3. As shown in Fig. 3, the persistence length reached a minimum value of 25 nm ± 6.5 nm at a concentration of 500 nM, which is about half of its size in an HU-free solution. Increasing the protein concentration further to 900 nM resulted in an increase of the persistence length to a value of 33 nm ± 1 nm. Further increase of the protein concentration up to 3 μM did not change the persistence length (Figs. 1–3).

Previous single-molecule studies mainly used magnetic tweezers. Two studies on *Eco*HU (14,15) showed a further increase of the persistence length to values that are larger than that measured for bare DNA, in contrast to our findings. Another study with an HU that is similar to the one we used (*Bst*HU) reported that there is no increase in the DNA

Please cite this article in press as: Nir et al., HU Protein Induces Incoherent DNA Persistence Length, Biophysical Journal (2011), doi:10.1016/j.bpj.2010.12.3687

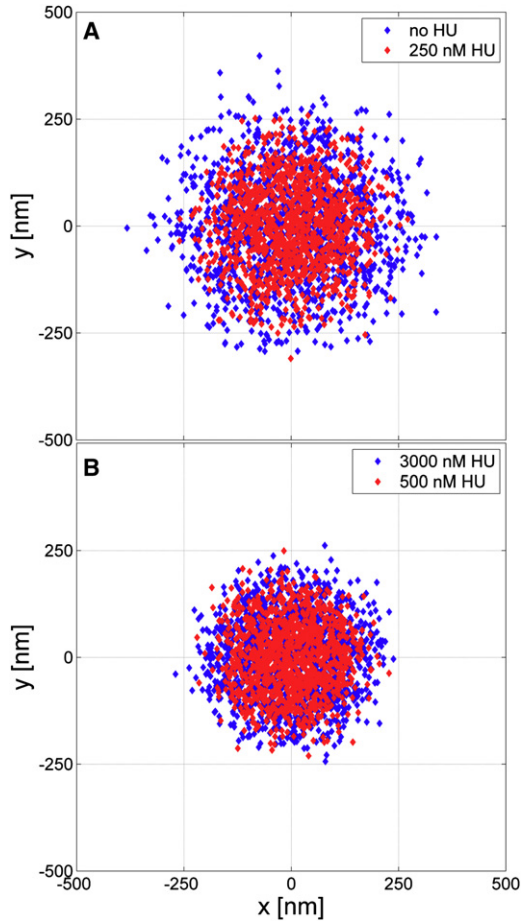

FIGURE 1 A comparison of the bead positions for different HU concentrations. (*A*) Comparison between naked DNA (no HU protein, *blue*) and a complex of DNA-250 nM HU protein (*red*). With 250 nM HU, the bead is restricted to a smaller volume, a result of the DNA compaction due to the binding of HU. (*B*) A comparison between complex of DNA-500 nM HU (*red*) and a complex of DNA-3000 nM HU protein (*blue*). With 500 nM HU, the bead is more confined. Apparently, when increasing the protein concentration above 500 nM, the persistence length of the DNA increases.

stiffening beyond the bare DNA levels (16), in agreement with our findings. Nevertheless, these measurements still used force-based methods.

AFM measurements of DNA on mica surface were performed after incubating it with HU concentrations of 0, 250, and 1000 nM (Fig. 4); see Materials and Methods for details. Fig. 4 *c* shows complexes of 1000 nM HU-DNA. Note that most of the segments along the DNA have a rather small curvature whereas few others have an abrupt large-angle curvature. This is in contrast to the HU-free DNA (Fig. 4 *a*) that shows a more uniform and small curvature distribution. We analyzed the angular distribution along the DNA for the different HU concentrations, which is identical to the curvature, up to a multiplication factor by the segment size.

After analyzing the angular distribution for 10 nm segments along the DNA, we calculated the CDF,

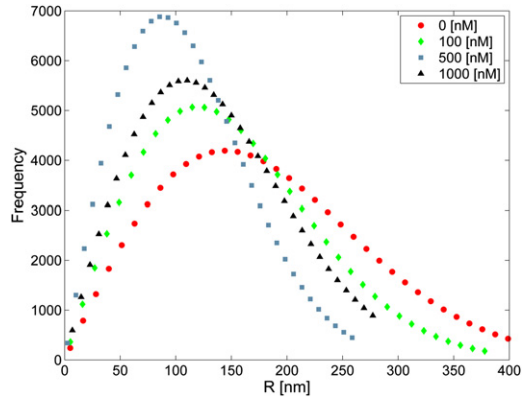

FIGURE 2 Comparison of the radial distributions of the bead position for different HU concentrations as measured for the same bead. Circles represent DNA without HU proteins and the persistence length is 50 nm. Diamonds are for DNA in a solution with a concentration of 100 nM HU. The distribution is narrower compared to the HU-free DNA and the persistence length is ~39 nm. Squares represent DNA with HU concentration of 500 nM and the distribution is narrower compared to the 100 nM distribution with a persistence length of ~26 nm. Triangles represent DNA with HU concentration of 1000 nM and the distribution is now wider than for 500 nM. The measured persistence length is ~34 nm.

$$CDF(\theta) = \int_0^{\theta} P(|\theta'|)d\theta'.$$

The CDF provides a clearer function for comparing the variations of the DNA conformation as a function of the HU concentrations, as it is less sensitive to high-frequency variation in the angular distribution function. Fig. 5 shows the CDF for the different HU concentrations we measured. The following results are observed by comparing the CDFs of the different HU concentrations:

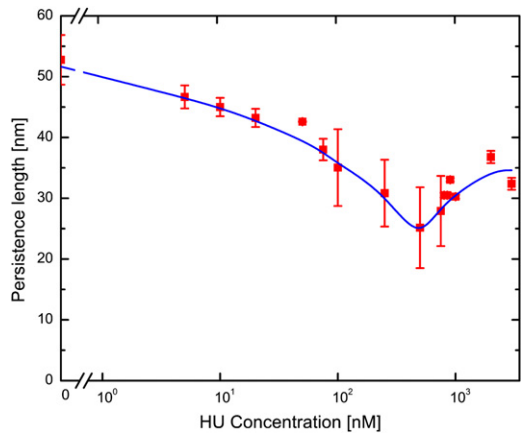

FIGURE 3 DNA persistence length dependence on HU protein concentration. The persistence length has a bimodal character. It initially decreases to a value of 25 nm at an HU concentration of 500 nM. It then increases and reaches a maximum value for HU concentration of 900 nM from which it does not change much when increasing the concentration further. The solid line is a guide to the eye.

Please cite this article in press as: Nir et al., HU Protein Induces Incoherent DNA Persistence Length, Biophysical Journal (2011), doi:10.1016/j.bpj.2010.12.3687

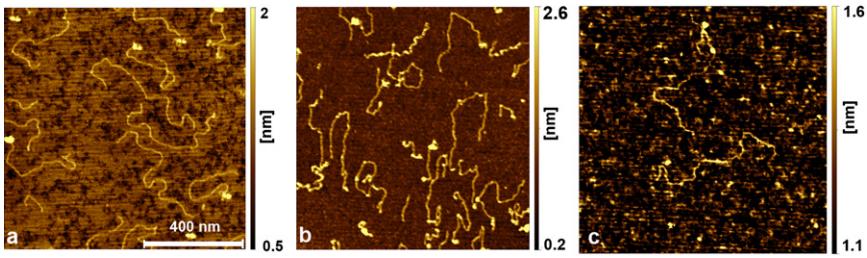

FIGURE 4 AFM imaging of HU-DNA complexes deposited on freshly cleaved mica. (*a*) Bare 2700-bp DNA. (*b*) DNA with 250 nM HU. (*c*) DNA with 1 μM HU. Image size was 1^2 μm^2 at 2048 $\times$ 2048 pixels.

1. The 250 nM HU-DNA complex has a smaller fraction of small-angles with respect to that of the 0 nM HU-DNA. It also means that there is a larger fraction of large-angles for the 250 nM DNA than the 0 nM DNA. For instance, 64.5% of the angles are $<15^\circ$ for the 250 nM complex compared to 70% for the HU-free DNA. It means that the curvature of the 250 nM HU-DNA contains a larger fraction of DNA segments that are more curved, and therefore results in a smaller persistence length.
2. There is a larger fraction of small-angles for the 1000 nM HU-DNA complex than for the HU-free DNA. For instance, 73.5% of the angles are $<15^\circ$ for the 1000 nM while it is only 70% for HU-free DNA (also refer to Fig. S3 and to the curvature distribution comparison section in the Supporting Material).

The curvature analysis shows that the end-to-end distance results from the interplay of two fractions of curvatures along the DNA. The differences in curvature distributions of the different HU-DNA complexes are relatively small and demonstrate that even few DNA segments with large bending angles can modify the effective persistence length. Moreover, at high concentrations, most of the DNA is relatively rigid (small curvature) and should lead to a large end-to-end distance and therefore large persistence length. Nevertheless, a few large bending sites reduce the end-to-end distance and leads to an overall normal persistence length, as was measured.

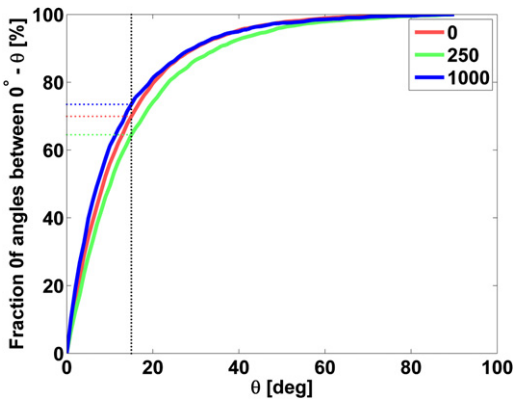

FIGURE 5 Cumulative distribution function for the angular distribution along the DNA calculated from each two segments located 10 nm apart at different concentrations of HU-free DNA, 250 nM HU-DNA, and 1000 nM HU-DNA. The latest has the narrowest angular distribution, whereas 250 nM has the broadest. The vertical dotted line is plotted at 15° and the horizontal lines crossing it show the related percentage for each concentration. For 1000 nM HU concentration, 73.5% of the angles up to 15° are accounted. This is larger than 70% for HU-free DNA and 64.5% for 250 nM HU concentration. The values are not very different, indicating that a few large bending points lead to significant changes in the DNA persistence length.

CONCLUSIONS

Our results confirmed the bimodal effect of HU on DNA (Figs. 1–3). At relatively low protein concentrations (up to 500 nM) we find a decreased persistence length, thus an increase in the DNA flexibility. However, above 500 nM the persistence length increases from 25 nm to ~35 nm. Previous data showed the bimodal character (14,15,17) with a dramatic increase of the persistence length to ~150 nm for HU concentration of 900 nM, three times larger than its value for DNA in physical conditions.

In contrast, we report on a more modest increase of the persistence length to a value that is 70% of its initial size. Reasonable explanations for the dissimilarity might evolve from the following:

1. The different nature of the TPM method used here versus the optical and magnetic tweezers methods that were used before. A previous study demonstrated that, for 150 mM salt concentration (higher salt concentration than was used here), a small shift in the applied force (from 0.1 pN to 0.3 pN) can drive unbinding of HU from DNA (18). Therefore, the TPM may give different results than the methods that use stretching forces that are applied on the DNA.
2. The use of HU protein from different bacteria (*Bst*HU instead of *Eco*HU). As was mentioned in Results and Discussion, a previous study with *Bst*HU showed no stiffening beyond bare DNA levels (16) and it was shown lately that properties of different HU homologs may vary (44). The difference between *Eco*HU and *Bst*HU may evolve from the differences in their binding-site sizes. For *Eco*HU, it was shown that binding-site size is decreased when increasing protein concentration,

Please cite this article in press as: Nir et al., HU Protein Induces Incoherent DNA Persistence Length, Biophysical Journal (2011), doi:10.1016/j.bpj.2010.12.3687

leading to DNA rigidification (27). Although there are no similar experimental results for *Bst*HU, it may have a different binding-site size with respect to *Eco*HU, leading to a different bending activity as a function of the protein's concentration.

The bimodality of HU together with the modest increase of the persistence length at high concentrations can be explained according to a model that was lately suggested. It assumes that the DNA is constructed from rigid segments and flexible joints (26). The model distinguishes two possible bending patterns along the polymer. If two neighboring segments are unoccupied by proteins, the bending angle θ is small, leading to the normal persistence length of DNA. When a protein occupies a segment without a neighboring protein, the spontaneous curvature increases and when proteins occupy both neighboring segments, the spontaneous curvature is reduced again. The model therefore predicts that the DNA contains bent joints (large spontaneous curvature) and unbent joints (small spontaneous curvature) along the same DNA strand.

An indication to that was observed previously by AFM (14). Certainly at low protein concentration, it is more likely to find single HU protein binding to the DNA and the DNA adopts a more flexible form as a result of few abrupt large-angle curvatures. When increasing the protein concentration, some of these large angle sites vanish as a result of HU proteins binding on neighboring segments, thus making the DNA stiffer again.

We also tested the possible fit of the curvature distribution according to the Gaussian random walk model, as suggested before (38). A good fit is achieved with a single Gaussian distribution for HU-free DNA or a relatively small HU concentration (250 nM). However, for the higher protein concentration (1000 nM), two Gaussians provided a more satisfying fit, indicating that there are two populations with small and large curvatures (see curvature distribution fitting in the Supporting Material).

The curvature analysis of the DNA strands as measured with the AFM strongly supports the model, and indicates that there is a significant percentage of large angle sites along the DNA. It also showed that the distribution of curvatures depends on the HU concentration, and the results on the HU concentrations of 0, 250, and 1000 nM are in line with the described model.

The results and model also emphasizes the limitations of measuring the persistence length alone, and the importance of the AFM data for providing not only the end-to-end distribution, but also the actual curvature distribution.

The TPM data demonstrates that it can be used for measuring the conformation and interactions of DNA with proteins in a similar manner to magnetic and optical tweezers. TPM is relatively simple to perform, and being a passive method, it can be used to observe dynamics of polymers without applying stretching forces.

What may be the biological implications of the HU-DNA bimodal character?

The small persistence length achieved with a low HU concentration indicates that even a low concentration can lead to high condensation of the DNA and enables an efficient packing of the chromosome. By changing the concentration of HU during the different cell phases, the bimodal effect provides a degree of freedom for the interplay of a more rigid form versus chromosome condensation.

In conclusion, by using TPM, which is a force-free single molecule technique, we have shown that varying the HU concentration induces a bimodal character on dsDNA in vitro. By combining the results with curvature analysis from AFM measurements, our data indicates the coexistence of stiffer and more flexible sites, and a delicate interplay in their ratios as a result of the HU concentration.

SUPPORTING MATERIAL

Three figures are available at http://www.biophysj.org/biophysj/supplemental/S0006-3495(10)05199-4.

With great pleasure we thank Gil Reuven, Noam Maoz, and Haim Cohen from Bar Ilan University for assisting in the molecular biology tasks. We thank Shay Rappaport and Yitzhak Rabin for stimulating discussions and enlightening comments. We also thank Shimon Filo from Bar Ilan University for the sample holder design and manufacturing.

This work was supported in part by the Israel Science Foundation grant Nos. 985/08, 1729/08, 1793/07, and 25/07.

REFERENCES

1. Thanbichler, M., S. C. Wang, and L. Shapiro. 2005. The bacterial nucleoid: a highly organized and dynamic structure. *J. Cell. Biochem.* 96:506–521.
2. Johnson, R. C., L. M. Johnson, …, J. F. Gardner. 2005. Major nucleoid proteins in the structure and function of the *Escherichia coli* chromosome. *In* The Bacterial Chromosome. N. P. Higgins, editor. ASM Press, Washington, DC. 65–132.
3. Stavans, J., and A. Oppenheim. 2006. DNA-protein interactions and bacterial chromosome architecture. *Phys. Biol.* 3:R1–R10.
4. Luijsterburg, M. S., M. C. Noom, …, R. T. Dame. 2006. The architectural role of nucleoid-associated proteins in the organization of bacterial chromatin: a molecular perspective. *J. Struct. Biol.* 156:262–272.
5. Krawiec, S., and M. Riley. 1990. Organization of the bacterial chromosome. *Microbiol. Rev.* 54:502–539.
6. Kamashev, D., and J. Rouviere-Yaniv. 2000. The histone-like protein HU binds specifically to DNA recombination and repair intermediates. *EMBO J.* 19:6527–6535.
7. Pinson, V., M. Takahashi, and J. Rouviere-Yaniv. 1999. Differential binding of the *Escherichia coli* HU, homodimeric forms and heterodimeric form to linear, gapped and cruciform DNA. *J. Mol. Biol.* 287:485–497.
8. Swinger, K. K., and P. A. Rice. 2007. Structure-based analysis of HU-DNA binding. *J. Mol. Biol.* 365:1005–1016.
9. Manna, D., and J. Gowrishankar. 1994. Evidence for involvement of proteins HU and RpoS in transcription of the osmoresponsive proU operon in *Escherichia coli*. *J. Bacteriol.* 176:5378–5384.
10. Oberto, J., S. Nabti, …, J. Rouviere-Yaniv. 2009. The HU regulon is composed of genes responding to anaerobiosis, acid stress, high osmolarity and SOS induction. *PLoS ONE.* 4:e4367.

11. Dixon, N. E., and A. Kornberg. 1984. Protein HU in the enzymatic replication of the chromosomal origin of *Escherichia coli*. *Proc. Natl. Acad. Sci. USA.* 81:424–428.
12. Grove, A., A. Galeone, …, E. P. Geiduschek. 1996. Localized DNA flexibility contributes to target site selection by DNA-bending proteins. *J. Mol. Biol.* 260:120–125.
13. Boubrik, F., and J. Rouviere-Yaniv. 1995. Increased sensitivity to γ irradiation in bacteria lacking protein HU. *Proc. Natl. Acad. Sci. USA.* 92:3958–3962.
14. van Noort, J., S. Verbrugge, …, R. T. Dame. 2004. Dual architectural roles of HU: formation of flexible hinges and rigid filaments. *Proc. Natl. Acad. Sci. USA.* 101:6969–6974.
15. Skoko, D., B. Wong, …, J. F. Marko. 2004. Micromechanical analysis of the binding of DNA-bending proteins HMGB1, NHP6A, and HU reveals their ability to form highly stable DNA-protein complexes. *Biochemistry.* 43:13867–13874.
16. Schnurr, B., C. Vorgias, and J. Stavans. 2006. Compaction and supercoiling of single, long DNA molecules by HU protein. *Biophys. Rev. Lett.* 1:29–44.
17. Sagi, D., N. Friedman, …, J. Stavans. 2004. Modulation of DNA conformations through the formation of alternative high-order HU-DNA complexes. *J. Mol. Biol.* 341:419–428.
18. Xiao, B., R. C. Johnson, and J. F. Marko. 2010. Modulation of HU-DNA interactions by salt concentration and applied force. *Nucleic Acids Res.* 38:6176–6185.
19. Neuman, K. C., and A. Nagy. 2008. Single-molecule force spectroscopy: optical tweezers, magnetic tweezers and atomic force microscopy. *Nat. Methods.* 5:491–505.
20. Gore, J., Z. Bryant, …, C. Bustamante. 2006. DNA overwinds when stretched. *Nature.* 442:836–839.
21. Woodside, M. T., C. García-García, and S. M. Block. 2008. Folding and unfolding single RNA molecules under tension. *Curr. Opin. Chem. Biol.* 12:640–646.
22. Bryant, Z., M. D. Stone, …, C. Bustamante. 2003. Structural transitions and elasticity from torque measurements on DNA. *Nature.* 424: 338–341.
23. Zhuang, X. 2004. Molecular biology. Unraveling DNA condensation with optical tweezers. *Science.* 305:188–190.
24. Lia, G., D. Bensimon, …, L. Finzi. 2003. Supercoiling and denaturation in Gal repressor/heat unstable nucleoid protein (HU)-mediated DNA looping. *Proc. Natl. Acad. Sci. USA.* 100:11373–11377.
25. Marko, J. F., and E. D. Siggia. 1997. Driving proteins off DNA using applied tension. *Biophys. J.* 73:2173–2178.
26. Rappaport, S. M., and Y. Rabin. 2008. Model of DNA bending by cooperative binding of proteins. *Phys. Rev. Lett.* 101:038101.
27. Koh, J., R. M. Saecker, and M. T. Record, Jr. 2008. DNA binding mode transitions of *Escherichia coli* HU($\alpha\beta$): evidence for formation of a bent DNA—protein complex on intact, linear duplex DNA. *J. Mol. Biol.* 383:324–346.
28. Czapla, L., D. Swigon, and W. K. Olson. 2008. Effects of the nucleoid protein HU on the structure, flexibility, and ring-closure properties of DNA deduced from Monte Carlo simulations. *J. Mol. Biol.* 382: 353–370.
29. Schafer, D. A., J. Gelles, …, R. Landick. 1991. Transcription by single molecules of RNA polymerase observed by light microscopy. *Nature.* 352:444–448.
30. Lindner, M., G. Nir, …, Y. Garini. 2009. Studies of single molecules in their natural form. *Isr. J. Chem.* 49:283–291.
31. Zurla, C., A. Franzini, …, L. Finzi. 2006. Novel tethered particle motion analysis of CI protein-mediated DNA looping in the regulation of bacteriophage-λ. *J. Phys. Condens. Matter.* 18:S225–S234.
32. Zurla, C., C. Manzo, …, L. Finzi. 2009. Direct demonstration and quantification of long-range DNA looping by the λ bacteriophage repressor. *Nucleic Acids Res.* 37:2789–2795.
33. Nelson, P. C., C. Zurla, …, D. Dunlap. 2006. Tethered particle motion as a diagnostic of DNA tether length. *J. Phys. Chem. B.* 110:17260–17267.
34. Beausang, J. F., C. Zurla, …, P. C. Nelson. 2007. Elementary simulation of tethered Brownian motion. *Am. J. Phys.* 75:520–523.
35. Pouget, N., C. Turlan, …, M. Chandler. 2006. IS911 transpososome assembly as analyzed by tethered particle motion. *Nucleic Acids Res.* 34:4313–4323.
36. Vanzi, F., L. Sacconi, and F. S. Pavone. 2007. Analysis of kinetics in noisy systems: application to single molecule tethered particle motion. *Biophys. J.* 93:21–36.
37. Lyubchenko, Y. L., and L. S. Shlyakhtenko. 1997. Visualization of supercoiled DNA with atomic force microscopy in situ. *Proc. Natl. Acad. Sci. USA.* 94:496–501.
38. Rivetti, C., M. Guthold, and C. Bustamante. 1996. Scanning force microscopy of DNA deposited onto mica: equilibration versus kinetic trapping studied by statistical polymer chain analysis. *J. Mol. Biol.* 264:919–932.
39. Rubinstein, M., and R. H. Colby. 2003. Polymer Physics. Oxford University Press, Oxford, UK.
40. Segall, D. E., P. C. Nelson, and R. Phillips. 2006. Volume-exclusion effects in tethered-particle experiments: bead size matters. *Phys. Rev. Lett.* 96:088306.
41. Wong, W. P., and K. Halvorsen. 2006. The effect of integration time on fluctuation measurements: calibrating an optical trap in the presence of motion blur. *Opt. Express.* 14:12517–12531.
42. Destainville, N., and L. Salomé. 2006. Quantification and correction of systematic errors due to detector time-averaging in single-molecule tracking experiments. *Biophys. J.* 90:L17–L19.
43. Padas, P. M., K. S. Wilson, and C. E. Vorgias. 1992. The DNA-binding protein HU from mesophilic and thermophilic bacilli: gene cloning, overproduction and purification. *Gene.* 117:39–44.
44. Grove, A. 2010. Functional evolution of bacterial histone-like HU proteins. *Curr. Issues Mol. Biol.* 13:1–12.